High-spin states in near-spherical ^{88}Y

C. J. Xu (徐长江),[1] S. Y. Wang (王守宇),[1,*] C. Y. Niu (牛晨阳),[1] C. Liu (刘晨),[1] B. Qi (亓斌),[1] D. P. Sun (孙大鹏),[1] L. Liu (刘雷),[1] P. Zhang (张盼),[1] Z. Q. Li (李志泉),[1] Z. Wang (王振),[1] X. G. Wu (吴晓光),[2] G. S. Li (李广生),[2] C. Y. He (贺创业),[2] Y. Zheng (郑云),[2] B. B. Yu (于蓓蓓),[2] C. B. Li (李聪博),[2] S. P. Hu (胡世鹏),[2] S. H. Yao (姚顺和),[2] X. P. Cao (曹雪鹏),[2] and J. L. Wang (汪金龙)[2]

[1]*Shandong Provincial Key Laboratory of Optical Astronomy and Solar-Terrestrial Environment, School of Space Science and Physics, Shandong University at Weihai, Weihai 264209, People's Republic of China*

[2]*China Institute of Atomic Energy, Beijing 102413, People's Republic of China*

(Received 18 June 2012; published 7 August 2012)

High-spin states in doubly odd ^{88}Y have been investigated using the ^{82}Se(^{11}B, 5n) reaction at beam energies of 48 and 52 MeV. On the basis of the γ-γ coincidence relationships, the level scheme of ^{88}Y has been extended up to an excitation energy of 9.5 MeV at spin 21$\hbar$. About 20 new levels and 30 new transitions have been added into the level scheme, and spin-parity assignments have been made to most of the newly proposed levels. In order to better understand the nuclear structure of ^{88}Y, semiempirical shell-model calculations were carried out considering a valence space formed by the proton $1p_{1/2}$, $1p_{3/2}$, $0f_{5/2}$, $0g_{9/2}$ and neutron $0g_{9/2}$ orbitals.

DOI: 10.1103/PhysRevC.86.027302 PACS number(s): 23.20.Lv, 21.60.Cs, 25.70.Gh, 27.50.+e

Nuclei in the $A \sim 80$ mass region have attracted considerable theoretical and experimental attention in recent years. These investigations have revealed a number of interesting nuclear structure phenomena, such as signature inversion [1], shape coexistence [2,3], magnetic rotation [4,5], and most recently the chiral doublet bands [6]. In this mass region, because of the $Z = 38$ subshell closure, the $^{88}_{38}$Sr$_{50}$ semimagic nucleus has been often used as a core for shell-model calculations. Therefore, studies of ^{88}Sr and its neighbors could not only provide important information about the single-particle energies but also the two-body matrix elements needed for microscopic calculations. The odd-odd nucleus $^{88}_{39}$Y$_{49}$ has one proton above the subshell closure at $Z = 38$ and one neutron hole above the shell closure at $N = 50$. Hence, it is interesting to study high-spin states of the odd-odd nucleus ^{88}Y. In this Brief Report, we report on new results for the odd-odd ^{88}Y through the heavy ion fusion-evaporation reaction ^{82}Se(^{11}B, 5n). Semiempirical shell-model calculations are used to interpret the level structures of ^{88}Y.

High-spin states in ^{88}Y were populated using the ^{82}Se(^{11}B, 5n) reaction at beam energies of 48 and 52 MeV. The ^{11}B beam was provided by the HI-13 tandem accelerator at the China Institute of Atomic Energy (CIAE) in Beijing with an intensity of six particles nA on the target. The target consisted of 1.35 mg/cm^2 of isotopically enriched ^{82}Se rolled onto a 9.1 mg/cm^2 Pb backing. The deexcitation γ rays were detected by an array of 12 Compton-suppressed HPGe detectors and two planar-type HPGe detectors. A total of 130×10^6 γ-γ coincidence events were collected when two or more detectors to be fired within 200 ns were accumulated in the event-by-event mode. All detectors were calibrated for γ-ray energies and efficiencies using the standard ^{152}Eu source placed at the target position. In the off-line analysis, the outputs of the array were then matched for gain and zero position. Then, all the coincidence events were recalibrated to 0.5 keV/channel and sorted into a 4096 by 4096 channel symmetrized E_γ-E_γ matrix. The multipolarities of the emitted γ rays were analyzed by means of angular distributions from oriented (ADO) states. The ADO ratio was defined as $I_\gamma(\text{at} \sim 45^\circ)/I_\gamma(\text{at} \sim 90^\circ)$. Here the γ-ray intensities (I_γ) were determined under the same gating conditions on the sum of all Ge detectors. By examining the strong γ rays with known multipolarities in ^{88}Sr [7], which were also produced in the present experiment, the ADO ratios for stretched quadrupole or $\Delta I = 0$ dipole radiations and stretched pure dipole transitions are found to be $\sim$1.3 and $\sim$0.7, respectively. The ADO ratios of most γ rays in ^{88}Y are shown in Fig. 1.

The level scheme of ^{88}Y developed in the present work is shown in Fig. 2. It is established up to $\sim$10 MeV excitation energy and 21$\hbar$ spin with the addition of about 30 new transitions to that reported earlier by Warburton *et al.* [8]. As shown in Fig. 2, the level scheme can be roughly separated into four parts, and they have been labeled on top of the level sequences with A, B, C, and D for convenience of discussion. The placement of γ rays in the level scheme is based upon their coincidence relationships, energy sums, and intensity balances. Typical prompt γ-γ coincidence spectra for ^{88}Y are shown in Fig. 3. The spin and parity assignments are based on ADO ratios of the γ rays as well as on deexcitation modes. We have confirmed almost all γ-rays placements in the previous work [8]. Extensions and alterations of the level scheme with respect to previous work are given in the following.

The cascade of γ rays labeled A in Fig. 2 was reported up to the 10^+ state [8]. All these transitions and their multipolarities were confirmed in this work. In addition, several new γ rays belonging to ^{88}Y were identified and found to be in coincidence with the 1769.4 keV transition deexciting the 10^+ state at 2443.9 keV, but not with the 1208.0 keV transition deexciting the 11^- state at 3651.9 keV. These γ rays have been placed on top of the 10^+ state at 2443.9 keV as given in Fig. 2. Spectra showing some of the new transitions are presented in Figs. 3(a) and 3(b). The ADO ratios and energy sum relationships of the involved transitions suggest spin and parity values of 11^+, 11^+,

*sywang@sdu.edu.cn

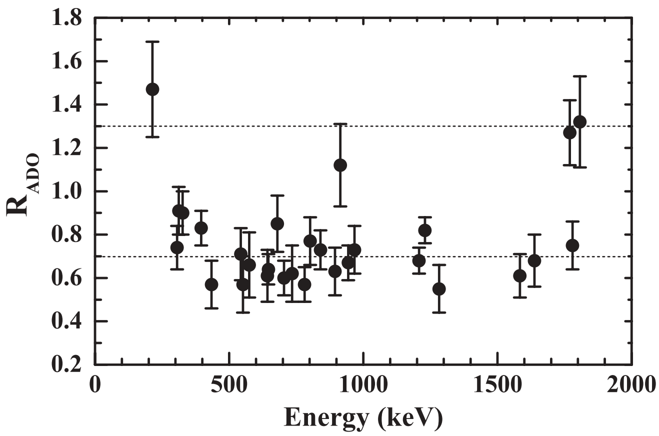

FIG. 1. The ADO values of transitions of ^{88}Y plotted as a function of the γ-ray energy. The dashed lines correspond to typical ADO values of stretched quadrupole transitions and stretched nonmixed dipole transitions.

12^+, 12^+, and 13^+ for the 3283.9, 3726.8, 4621.3, 4967.9, and 5264.3 keV levels, respectively.

The sequence of negative-parity yrast states (level sequence B) has been known up to the state at 5558.0 keV [8]. In Ref. [8], tentative spin assignments of 14 and 15 were proposed for the levels at 4823.7 and 5558.0 keV, respectively. However, no parity assignments were given for the two levels. In the present work, a mixed $M1/E2$ character was obtained for the 734.3 and 646.0 keV transitions from our experimental data. In addition, Warburton *et al.* [8] assigned $\Delta I = 1 M1/E2$ multipolarity to the 213.8 keV transition, while we proposed an $E2$ character for this γ ray based on the present measured ADO ratios. Taking the above information into account, the 4177.7, 4823.7, and 5558.0 keV levels are suggested as the spin-parity of $(14)^-$, $(15)^-$, and $(16)^-$, respectively.

On the left-hand side of the level scheme in Fig. 2, a new cascade of γ rays with energies of 551.2, 326.5, 704.5, and 781.2 keV was identified and labeled with C. Figure 3(c) presents a spectrum gated by the 326.5 keV transition; one can see most of the corresponding coincidence γ peaks shown in Fig. 2. Level sequence C depopulated a negative-parity yrast sequence via three linking transitions 1584.0, 1991.8, and 2086.6 keV. Owing to the poor statistics, the ADO ratio of the only 1584.0 keV transition can be obtained. Its ADO ratio was determined to be ~0.61, indicating that the 1584.0 keV γ ray corresponds to a mixed $M1/E2$ transition with a negative mixing ratio. This leads the spin and parity assignment to $I^\pi = 17^-$ for the 7142.0 keV level.

Above the 16^- state, another transition sequence (D) consisting of 305.6, 434.2, 543.0, and 574.5 keV γ rays was observed and placed on the right-hand side of the level scheme. The ADO ratio analysis shows that they have stretched dipole characters. Figure 3(d) presents a spectrum gated by the 305.6 keV transition. The ordering of γ rays and the spin-parity assignments in the level sequence D are based on level structure systematics and the following theoretical considerations. It is noted that the present placement for the sequences D doesn't achieve a satisfactory intensity balance, which imply missing connecting transitions between sequences D and B. The missing connecting transitions may be high-energy γ rays, or due to a decay branching through several cascades each of which is too weak to be observed.

The nucleus ^{88}Y has one proton above the level gap at $Z = 38$ and one neutron hole in the $N = 50$ shell. The level scheme of ^{88}Y exhibits a rather irregular structure. It indicates that ^{88}Y is a nearly spherical nucleus where multiparticle excitations dominate. Therefore, we discuss these structures on the basis of the shell model framework. Large-scale shell-model calculations [8] were previously carried out to interpret the low-lying excited states in ^{88}Y. In order to determine the configuration and better understand the high-spin states of ^{88}Y observed in the present work, we have performed semiempirical shell-model (SESM) calculations. The detailed formalism can be found in Ref. [9] and references therein. In this approach, level energies of multi-ph configurations are calculated using nuclear ground state masses, single-particle energies, and two-particle interactions obtained from experimental data in the neighboring nuclei. In our calculation, the $^{88}_{38}$Sr$_{50}$ was chosen as the core. The calculations were performed in the model space $\pi(1p_{1/2},\ 1p_{3/2},\ 0f_{5/2},\ 0g_{9/2})\nu(0g_{9/2})$. Only two-body interactions were taken into account since a complex matrix element can be decomposed into a combination of two-body matrix elements. The single particle energies and the residual interaction strength were extracted from the neighboring nuclei [7,10–18]. The calculated level energies are listed in Table I, together with the corresponding configurations of the levels. In addition, calculated energy levels for ^{88}Y are compared with the experimental ones in Fig. 4 for the positive- and negative-parity states. From Table I and Fig. 4, the agreement between calculation and experiment is satisfactory for both the positive- and negative-parity states. The SESM calculation reproduces well not only the yrast levels (I_1) but also some nonyrast levels (I_2) except that the 12^-_1 state lies lower than the 11^-_1 state in the calculated results.

The low-lying states of ^{88}Y originate primarily due to the coupling of a one proton particle with a one neutron hole outside the $^{88}_{38}$Sr$_{50}$ core. From the early studies [19,20], the 4^- ground state and 5^- state were thought to arise from the $\pi p_{1/2} \otimes \nu g^{-1}_{9/2}$ multiplet. According to our SESM calculations, the yrast 6^- state may be interpreted as the core excitations of 2^+ coupling to $\pi p_{1/2} \otimes \nu g^{-1}_{9/2}$. The low-lying excited states with $I^\pi = 8^+$ and 9^+ have been suggested as members of the $\pi g_{9/2} \otimes \nu g^{-1}_{9/2}$ multiplet [19,20]. Based on the same argument, the next 10^+, 11^+, 10^-, and 11^- states are expected to originate from the $(\pi g_{9/2} \otimes \nu g^{-1}_{9/2}; 8^+) \otimes (^{88}Sr; 2^+)$, $(\pi g_{9/2} \otimes \nu g^{-1}_{9/2}; 9^+) \otimes (^{88}Sr; 2^+)$, $(\pi g_{9/2} \otimes \nu g^{-1}_{9/2}; 7^+) \otimes (^{88}Sr; 3^-)$, and $(\pi g_{9/2} \otimes \nu g^{-1}_{9/2}; 8^+) \otimes (^{88}Sr; 3^-)$ configurations, respectively. From Table I and Fig. 4, it can be seen that the calculated excitation energy for 10^+, 11^+, 10^-, and 11^- states are close to the experimental ones, thereby supporting the present configuration assignments.

For the states above the $11\hbar$, the excitation of proton particles from the inner core is suggested in the calculations, since the $Z = 38$ proton shell closure is much weaker than the $N = 50$ neutron shell closure. Therefore, the positive parity 12^+_1, 12^+_2, and 13^+ states of level sequence A are likely to

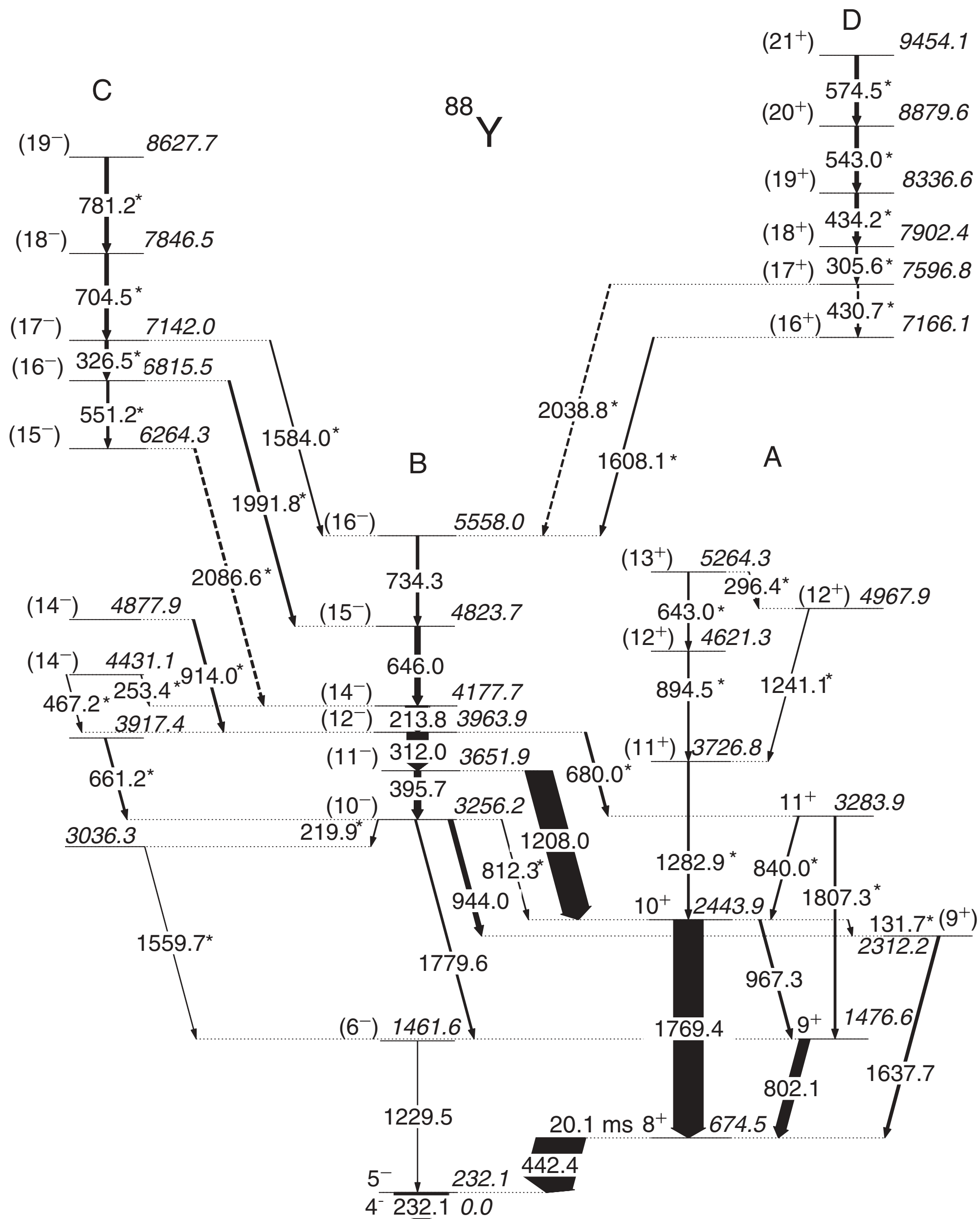

FIG. 2. Level scheme of ^{88}Y proposed in the present work. New transitions observed in the present work are denoted with asterisks.

result from configurations such as $\pi f_{5/2}^{-1} p_{1/2} g_{9/2} \otimes \nu g_{9/2}^{-1}$ and $\pi g_{9/2}^3 \otimes \nu g_{9/2}^{-1}$. Possible configurations for the negative parity states 12^-, 14_1^-, 14_2^-, and 15_1^- of level sequence B are the $\pi p_{3/2}^{-1} g_{9/2}^2 \otimes \nu g_{9/2}^{-1}$ and $\pi f_{5/2}^{-1} g_{9/2}^2 \otimes \nu g_{9/2}^{-1}$ multiplets.

As an example, the energy of the 14_1^- fully aligned state is calculated as

$$
\begin{aligned}
&E^{^{88}Y}_{(\pi p_{3/2}^{-1} g_{9/2}^2 \otimes \nu g_{9/2}^{-1};14^-)} \\
&= E^{^{89}Y}_{(\pi p_{3/2}^{-1} g_{9/2}^2;\frac{19}{2}^-)} + E^{^{87}Sr}_{(\nu g_{9/2}^{-1};\frac{9}{2}^+)} + \Delta\left(\pi p_{3/2}^{-1} \otimes \nu g_{9/2}^{-1}; 6^-\right) \\
&\quad + \Delta\left(\pi g_{9/2} \otimes \nu g_{9/2}^{-1}; 9^+\right) + \Delta\left(\pi g_{9/2} \otimes \nu g_{9/2}^{-1}; 8^+\right) + S \\
&= 4130.8 \text{ keV},
\end{aligned}
\tag{1}
$$

where E is the corresponding level energy and Δ is the two-body interaction between the two valence nucleons and can be directly extracted from the neighboring nuclei as follows:

$$
\begin{aligned}
&\Delta\left(\pi p_{3/2}^{-1} \otimes \nu g_{9/2}^{-1}; 6^-\right) \\
&\quad + \Delta\left(\pi g_{9/2} \otimes \nu g_{9/2}^{-1}; 9^+\right) + \Delta\left(\pi g_{9/2} \otimes \nu g_{9/2}^{-1}; 8^+\right) \\
&\quad = E^{^{90}Nb}_{(\pi p_{3/2}^{-1} g_{9/2}^2 \otimes \nu g_{9/2}^{-1};14^-)} - E^{^{91}Nb}_{(\pi p_{3/2}^{-1} g_{9/2}^2;\frac{19}{2}^-)} - E^{^{89}Zr}_{(\nu g_{9/2}^{-1};\frac{9}{2}^+)} - S' \\
&\quad = -346.6 \text{ keV}.
\end{aligned}
\tag{2}
$$

In this case, the binding energy terms are calculated to be

$$
\begin{aligned}
S &= B(^{88}Sr) + B(^{88}Y) - B(^{87}Sr) - B(^{89}Y), \\
S' &= B(^{90}Zr) + B(^{90}Nb) - B(^{91}Nb) - B(^{89}Zr),
\end{aligned}
\tag{3}
$$

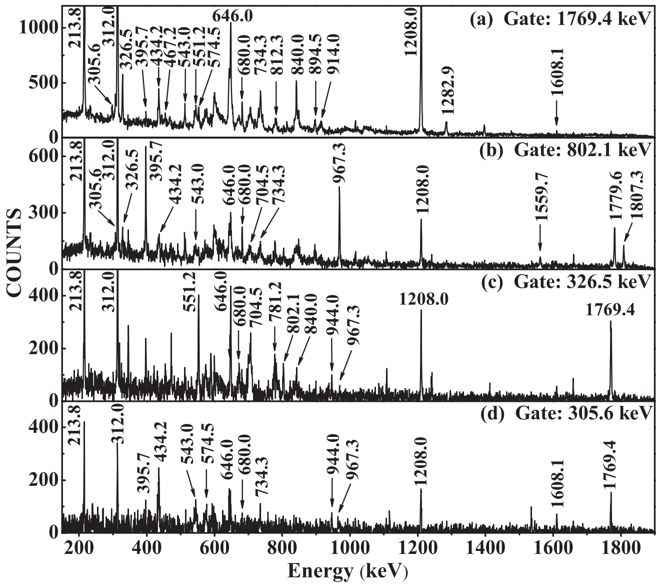

FIG. 3. Spectra of γ rays gated on the 1769.4, 802.1, 305.6, and 326.5 keV transitions, respectively.

where the $B(X)$ is the binding energy of the nucleus. $B(X)$ values can be found in Ref. [21]. The calculated excitation energy of 4130.8 keV is in good agreement with the experimental observation of $E(14_1^-) = 4177.7$ keV. In addition, the large-scale shell-model calculations in Ref. [8] also predicted a yrast 14^- state lying at 4107 keV. These results again confirm the present 14^- assignment for the level at 4177.7 keV.

TABLE I. Dominant configurations proposed from the semiempirical shell-model calculations of the high-spin states in ^{88}Y, together with the calculated level energies.

J^π	E_{exp}(keV)	Configuration	E_{cal}(keV)
8^+	674.5	$\pi g_{9/2} \otimes \nu g_{9/2}^{-1}$	625.9
9_1^+	1476.6	$\pi g_{9/2} \otimes \nu g_{9/2}^{-1}$	1438.9
10^+	2443.9	$(\pi g_{9/2} \otimes \nu g_{9/2}^{-1}; 8^+) \otimes 2^+$	2513.5
11_1^+	3283.9	$(\pi g_{9/2} \otimes \nu g_{9/2}^{-1}; 9^+) \otimes 2^+$	3326.9
12_1^+	4621.3	$\pi f_{5/2}^{-1} p_{1/2} g_{9/2} \otimes \nu g_{9/2}^{-1}$	4121.5
12_2^+	4967.9	$\pi g_{9/2}^3 \otimes \nu g_{9/2}^{-1}$	4916.1
13^+	5264.3	$\pi g_{9/2}^3 \otimes \nu g_{9/2}^{-1}$	5021.9
16^+	7166.1	$\pi g_{9/2}^5 \otimes \nu g_{9/2}^{-1}$	7078.1
17^+	7596.8	$\pi g_{9/2}^5 \otimes \nu g_{9/2}^{-1}$	7625.8
18^+	7902.4	$\pi f_{5/2}^{-1} p_{1/2}^{-1} g_{9/2}^3 \otimes \nu g_{9/2}^{-1}$	8241.7
6^-	1461.6	$(\pi p_{1/2} \otimes \nu g_{9/2}^{-1}; 4^-) \otimes 2^+$	1385.3
10^-	3256.2	$(\pi g_{9/2} \otimes \nu g_{9/2}^{-1}; 7^+) \otimes 3^-$	3577.4
11^-	3651.9	$(\pi g_{9/2} \otimes \nu g_{9/2}^{-1}; 8^+) \otimes 3^-$	3945.8
12^-	3963.9	$\pi p_{3/2}^{-1} g_{9/2}^2 \otimes \nu g_{9/2}^{-1}$	3646.4
14_1^-	4177.7	$\pi p_{3/2}^{-1} g_{9/2}^2 \otimes \nu g_{9/2}^{-1}$	4130.8
14_2^-	4431.1	$\pi f_{5/2}^{-1} g_{9/2}^2 \otimes \nu g_{9/2}^{-1}$	4224.1
15_1^-	4823.7	$\pi f_{5/2}^{-1} g_{9/2}^2 \otimes \nu g_{9/2}^{-1}$	5104.6
16_1^-	5558.0	$\pi p_{1/2}^{-1} g_{9/2}^4 \otimes \nu g_{9/2}^{-1}$	[a]

[a]The energy of the state has not been extracted because of the absence of the $\frac{25}{2}^-$ state in neighbor nuclei ^{89}Y.

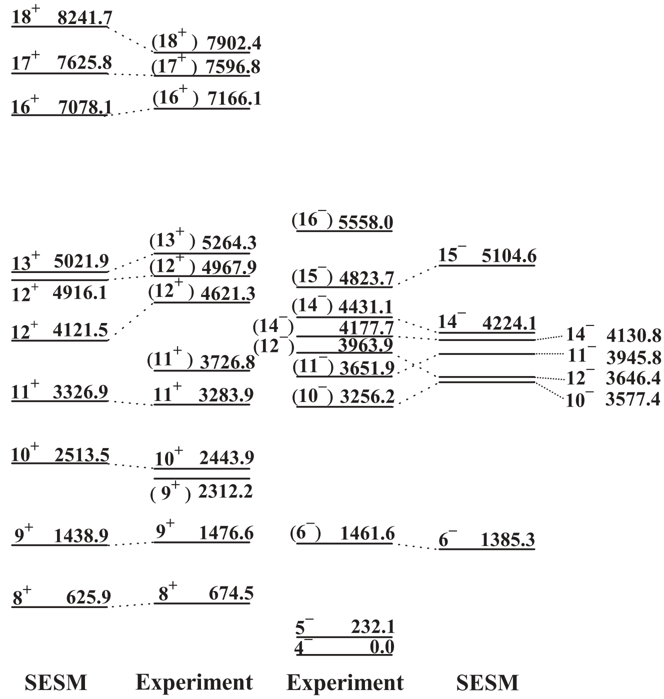

FIG. 4. Calculated positive- and negative-parity levels of ^{88}Y, which are compared with experimental ones.

Level sequence D is interesting in the present work, due to the fact that it consists of a bandlike structure between spins 17^+ and 21^+. These levels are connected by $\Delta I = 1$ stretched magnetic transitions; no crossover $E2$ transition has been observed. Similar positive parity structures were also systematically observed in the neighboring ^{86}Y [22], ^{89}Y [10], and ^{90}Y [23] nuclei at around $E_X \sim 7$ MeV. As shown in Fig. 2, level sequence D depopulated the negative-parity yrast sequence via high energy linking transitions. It is indicative of the excitation of nucleons across the shell gaps. Thus, six-quasiparticle configurations were proposed to the level sequence D. If we adopted the configurations of $(\pi g_{9/2}^5 \otimes \nu g_{9/2}^{-1})_{16^+}$ and $(\pi g_{9/2}^5 \otimes \nu g_{9/2}^{-1})_{17^+}$ for the 7166.1 keV and 7596.8 keV levels, one can find the present SESM calculations agree surprisingly well with experiment (see Table I or Fig. 4). With these features in mind, we propose that the 7166.1 keV and 7596.8 keV levels arise from the $(\pi g_{9/2}^5 \otimes \nu g_{9/2}^{-1})_{16^+,17^+}$ multiplet, leading to the spin-parity assignments of Fig. 2. However, it must be stressed that these assignments for level sequence D are tentative. For higher spin states, the SESM calculations of these levels were not done because of the absence of the level information in neighboring nuclei.

In summary, high-spin states in ^{88}Y were populated using the ^{82}Se(^{11}B, 5n) reaction at beam energies of 48 and 52 MeV. The level scheme of ^{88}Y has been extended up to an ∼10 MeV excitation energy and a 21$\hbar$ spin with the addition of about 30 new transitions. The level structure of ^{88}Y shows characteristics of a spherical nucleus and can be reasonably well understood within semiempirical shell-model calculations. Based on the SESM calculations, the low-lying states of ^{88}Y originate from the coupling of a one proton particle with a one neutron hole outside the $^{88}_{38}Sr_{50}$ core. For $I \geqslant 12\hbar$, most of the excited states are interpreted to involve two or four protons to be promoted across the $Z = 38$ gap.

The authors express their sincere gratitude to Professor S. M. Wyngaardt for reading and correcting this manuscript. This study is supported by the National Natural Science Foundation (Grants No. 11175108 and No. 11005069), the Shandong Natural Science Foundation (Grant No. ZR2010AQ005), and the Independent Innovation Foundation of Shandong University (Grant No. 2011ZRYQ004) of China.

[1] C. Plettner *et al.*, Phys. Rev. Lett. **85**, 2454 (2000).
[2] J. Ljungvall *et al.*, Phys. Rev. Lett. **100**, 102502 (2008).
[3] R. Wadsworth *et al.*, Phys. Lett. B **701**, 306 (2011).
[4] H. Schnare *et al.*, Phys. Rev. Lett. **82**, 4408 (1999).
[5] R. Schwengner *et al.*, Phys. Rev. C **66**, 024310 (2002).
[6] S. Y. Wang *et al.*, Phys. Lett. B **703**, 40 (2011).
[7] E. A. Stefanova, R. Schwengner, J. Reif, H. Schnare, F. Dönau, M. Wilhelm, A. Fitzler, S. Kasemann, P. vonBrentano, and W. Andrejtscheff, Phys. Rev. C **62**, 054314 (2000).
[8] E. K. Warburton, J. W. Olness, C. J. Lister, J. A. Becker, and S. D. Bloom, J. Phys. **G12**, 1017 (1986).
[9] J. Blomqvist and L. Rydström, Phys. Scr. **31**, 31 (1985).
[10] L. Funke *et al.*, Nucl. Phys. A **541**, 241 (1992).
[11] S. E. Arnell, A. Nilsson, and O. Stankiewicz, Nucl. Phys. A. **241**, 109 (1975).
[12] C. A. Fields, F. W. N. De Boer, J. J. Kraushaar, R. A. Ristinen, L. E. Samuelson, and E. Sugarbaker, Nucl. Phys. A **363**, 311 (1981).
[13] X. Z. Cui *et al.*, Phys. Rev. C **72**, 044322 (2005).
[14] A. Chakraborty *et al.*, Phys. Rev. C **72**, 054309 (2005).
[15] C. Y. He *et al.*, Chin. Phys. Lett. **27**, 102104 (2010).
[16] Coral M. Baglin, Nucl. Data Sheets. **86**, 1 (1999).
[17] G. Winter, R. Schwengner, J. Reif, H. Prade, J. Döring, R. Wirowski, N. Nicolay, P. von Brentano, H. Grawe, and R. Schubart, Phys. Rev. C **49**, 2427 (1994).
[18] N. Fotiades *et al.*, Phys. Rev. C **71**, 064312 (2005).
[19] J. R. Comfort and J. P. Schiffer, Phys. Rev. C **4**, 803 (1971).
[20] F. Gabbard, G. Chenevert, and K. K. Sekharan, Phys. Rev. C **6**, 2167 (1972).
[21] G. Audi, A. H. Wapstra, and C. Thibault, Nucl. Phys. A **729**, 337 (2003).
[22] C. Rusu *et al.*, Nucl. Phys. A **818**, 1 (2009).
[23] G. Rainovski *et al.*, Phys. Rev. C **65**, 044327 (2002).